

Cross Section for b -Jet Production in $\bar{p}p$ Collisions at $\sqrt{s} = 1.8$ TeV

B. Abbott,⁵⁰ M. Abolins,⁴⁷ V. Abramov,²³ B. S. Acharya,¹⁵ D. L. Adams,⁵⁷ M. Adams,³⁴ G. A. Alves,² N. Amos,⁴⁶ E. W. Anderson,³⁹ M. M. Baarmand,⁵² V. V. Babintsev,²³ L. Babukhadia,⁵² A. Baden,⁴³ B. Baldin,³³ P. W. Balm,¹⁸ S. Banerjee,¹⁵ J. Bantly,⁵⁶ E. Barberis,²⁶ P. Baringer,⁴⁰ J. F. Bartlett,³³ U. Bassler,¹¹ A. Bean,⁴⁰ M. Begel,⁵¹ A. Belyaev,²² S. B. Beri,¹³ G. Bernardi,¹¹ I. Bertram,²⁴ A. Besson,⁹ V. A. Bezzubov,²³ P. C. Bhat,³³ V. Bhatnagar,¹³ M. Bhattacharjee,⁵² G. Blazey,³⁵ S. Blessing,³¹ A. Boehnlein,³³ N. I. Bojko,²³ F. Borchering,³³ A. Brandt,⁵⁷ R. Breedon,²⁷ G. Briskin,⁵⁶ R. Brock,⁴⁷ G. Brooijmans,³³ A. Bross,³³ D. Buchholz,³⁶ M. Buehler,³⁴ V. Buescher,⁵¹ V. S. Burtovoi,²³ J. M. Butler,⁴⁴ F. Canelli,⁵¹ W. Carvalho,³ D. Casey,⁴⁷ Z. Casilum,⁵² H. Castilla-Valdez,¹⁷ D. Chakraborty,⁵² K. M. Chan,⁵¹ S. V. Chekulaev,²³ D. K. Cho,⁵¹ S. Choi,³⁰ S. Chopra,⁵³ J. H. Christenson,³³ M. Chung,³⁴ D. Claes,⁴⁸ A. R. Clark,²⁶ J. Cochran,³⁰ L. Coney,³⁸ B. Connolly,³¹ W. E. Cooper,³³ D. Coppers,⁴⁰ M. A. C. Cummings,³⁵ D. Cutts,⁵⁶ O. I. Dahl,²⁶ G. A. Davis,⁵¹ K. Davis,²⁵ K. De,⁵⁷ K. Del Signore,⁴⁶ M. Demarteau,³³ R. Demina,⁴¹ P. Demine,⁹ D. Denisov,³³ S. P. Denisov,²³ S. Desai,⁵² H. T. Diehl,³³ M. Diesburg,³³ G. Di Loreto,⁴⁷ S. Doulas,⁴⁵ P. Draper,⁵⁷ Y. Ducros,¹² L. V. Dudko,²² S. Duensing,¹⁹ S. R. Dugad,¹⁵ A. Dyshkant,²³ D. Edmunds,⁴⁷ J. Ellison,³⁰ V. D. Elvira,³³ R. Engelmann,⁵² S. Eno,⁴³ G. Eppley,⁵⁹ P. Ermolov,²² O. V. Eroshin,²³ J. Estrada,⁵¹ H. Evans,⁴⁹ V. N. Evdokimov,²³ T. Fahland,²⁹ S. Feher,³³ D. Fein,²⁵ T. Ferbel,⁵¹ H. E. Fisk,³³ Y. Fisyak,⁵³ E. Flattum,³³ F. Fleuret,²⁶ M. Fortner,³⁵ K. C. Frame,⁴⁷ S. Fuess,³³ E. Gallas,³³ A. N. Galyaev,²³ P. Gartung,³⁰ V. Gavrilov,²¹ R. J. Genik II,²⁴ K. Genser,³³ C. E. Gerber,³⁴ Y. Gershtein,⁵⁶ B. Gibbard,⁵³ R. Gilmartin,³¹ G. Ginter,⁵¹ B. Gómez,⁵ G. Gómez,⁴³ P. I. Goncharov,²³ J. L. González Solís,¹⁷ H. Gordon,⁵³ L. T. Goss,⁵⁸ K. Gounder,³⁰ A. Goussiou,⁵² N. Graf,⁵³ G. Graham,⁴³ P. D. Grannis,⁵² J. A. Green,³⁹ H. Greenlee,³³ S. Grinstein,¹ L. Groer,⁴⁹ P. Grudberg,²⁶ S. Grünendahl,³³ A. Gupta,¹⁵ S. N. Gurzhiev,²³ G. Gutierrez,³³ P. Gutierrez,⁵⁵ N. J. Hadley,⁴³ H. Haggerty,³³ S. Hagopian,³¹ V. Hagopian,³¹ K. S. Hahn,⁵¹ R. E. Hall,²⁸ P. Hanlet,⁴⁵ S. Hansen,³³ J. M. Hauptman,³⁹ C. Hays,⁴⁹ C. Hebert,⁴⁰ D. Hedin,³⁵ A. P. Heinson,³⁰ U. Heintz,⁴⁴ T. Heuring,³¹ R. Hirosky,³⁴ J. D. Hobbs,⁵² B. Hoeneisen,⁸ J. S. Hoftun,⁵⁶ S. Hou,⁴⁶ Y. Huang,⁴⁶ A. S. Ito,³³ S. A. Jerger,⁴⁷ R. Jesik,³⁷ K. Johns,²⁵ M. Johnson,³³ A. Jonckheere,³³ M. Jones,³² H. Jöstlein,³³ A. Juste,³³ S. Kahn,⁵³ E. Kajfasz,¹⁰ D. Karmanov,²² D. Karmgard,³⁸ R. Kehoe,³⁸ S. K. Kim,¹⁶ B. Klima,³³ C. Klopfenstein,²⁷ B. Knuteson,²⁶ W. Ko,²⁷ J. M. Kohli,¹³ A. V. Kostitskiy,²³ J. Kotcher,⁵³ A. V. Kotwal,⁴⁹ A. V. Kozelov,²³ E. A. Kozlovsky,²³ J. Krane,³⁹ M. R. Krishnaswamy,¹⁵ S. Krzywdzinski,³³ M. Kubantsev,⁴¹ S. Kuleshov,²¹ Y. Kulik,⁵² S. Kunori,⁴³ V. E. Kuznetsov,³⁰ G. Landsberg,⁵⁶ A. Leflat,²² F. Lehner,³³ J. Li,⁵⁷ Q. Z. Li,³³ J. G. R. Lima,³ D. Lincoln,³³ S. L. Linn,³¹ J. Linnemann,⁴⁷ R. Lipton,³³ A. Lucotte,⁵² L. Lueking,³³ C. Lundstedt,⁴⁸ A. K. A. Maciel,³⁵ R. J. Madaras,²⁶ V. Manankov,²² H. S. Mao,⁴ T. Marshall,³⁷ M. I. Martin,³³ R. D. Martin,³⁴ K. M. Mauritz,³⁹ B. May,³⁶ A. A. Mayorov,³⁷ R. McCarthy,⁵² J. McDonald,³¹ T. McMahon,⁵⁴ H. L. Melanson,³³ X. C. Meng,⁴ M. Merkin,²² K. W. Merritt,³³ C. Miao,⁵⁶ H. Miettinen,⁵⁹ D. Mihalea,⁵⁵ A. Mincer,⁵⁰ C. S. Mishra,³³ N. Mokhov,³³ N. K. Mondal,¹⁵ H. E. Montgomery,³³ R. W. Moore,⁴⁷ M. Mostafa,¹ H. da Motta,² E. Nagy,¹⁰ F. Nang,²⁵ M. Narain,⁴⁴ V. S. Narasimham,¹⁵ H. A. Neal,⁴⁶ J. P. Negret,⁵ S. Negroni,¹⁰ D. Norman,⁵⁸ L. Oesch,⁴⁶ V. Oguri,³ B. Olivier,¹¹ N. Oshima,³³ P. Padley,⁵⁹ L. J. Pan,³⁶ A. Para,³³ N. Parashar,⁴⁵ R. Partridge,⁵⁶ N. Parua,⁹ M. Paterno,⁵¹ A. Patwa,⁵² B. Pawlik,²⁰ J. Perkins,⁵⁷ M. Peters,³² O. Peters,¹⁸ R. Piegai,¹ H. Piekarczyk,³¹ B. G. Pope,⁴⁷ E. Popkov,³⁸ H. B. Prosper,³¹ S. Protopopescu,⁵³ J. Qian,⁴⁶ P. Z. Quintas,³³ R. Raja,³³ S. Rajagopalan,⁵³ E. Ramberg,³³ P. A. Rapidis,³³ N. W. Reay,⁴¹ S. Reucroft,⁴⁵ J. Rha,³⁰ M. Rijssenbeek,⁵² T. Rockwell,⁴⁷ M. Roco,³³ P. Rubinov,³³ R. Ruchti,³⁸ J. Rutherford,²⁵ A. Santoro,² L. Sawyer,⁴² R. D. Schamberger,⁵² H. Schellman,³⁶ A. Schwartzman,¹ J. Sculli,⁵⁰ N. Sen,⁵⁹ E. Shabalina,²² H. C. Shankar,¹⁵ R. K. Shivpuri,¹⁴ D. Shpakov,⁵² M. Shupe,²⁵ R. A. Sidwell,⁴¹ V. Simak,⁷ H. Singh,³⁰ J. B. Singh,¹³ V. Sirotenko,³³ P. Slattery,⁵¹ E. Smith,⁵⁵ R. P. Smith,³³ R. Snihur,³⁶ G. R. Snow,⁴⁸ J. Snow,⁵⁴ S. Snyder,⁵³ J. Solomon,³⁴ V. Sorín,¹ M. Sosebee,⁵⁷ N. Sotnikova,²² K. Soustruznik,⁶ M. Souza,² N. R. Stanton,⁴¹ G. Steinbrück,⁴⁹ R. W. Stephens,⁵⁷ M. L. Stevenson,²⁶ F. Stichelbaut,⁵³ D. Stoker,²⁹ V. Stolin,²¹ D. A. Stoyanova,²³ M. Strauss,⁵⁵ K. Streets,⁵⁰ M. Strovink,²⁶ L. Stutte,³³ A. Sznajder,³ W. Taylor,⁵² S. Tentindo-Repond,³¹ J. Thompson,⁴³ D. Toback,⁴³ S. M. Tripathi,²⁷ T. G. Trippe,²⁶ A. S. Turcot,⁵³ P. M. Tuts,⁴⁹ P. van Gemmeren,³³ V. Vaniev,²³ R. Van Kooten,³⁷ N. Varelas,³⁴ A. A. Volkov,²³ A. P. Vorobiev,²³ H. D. Wahl,³¹ H. Wang,³⁶ Z.-M. Wang,⁵² J. Warchol,³⁸ G. Watts,⁶⁰ M. Wayne,³⁸ H. Weerts,⁴⁷ A. White,⁵⁷ J. T. White,⁵⁸ D. Whiteson,²⁶ J. A. Wightman,³⁹ D. A. Wijngaarden,¹⁹ S. Willis,³⁵ S. J. Wimpenny,³⁰ J. V. D. Wirjawan,⁵⁸ J. Womersley,³³ D. R. Wood,⁴⁵ R. Yamada,³³ P. Yamin,⁵³ T. Yasuda,³³ K. Yip,³³ S. Youssef,³¹ J. Yu,³³ Z. Yu,³⁶ M. Zanabria,⁵ H. Zheng,³⁸ Z. Zhou,³⁹ Z. H. Zhu,⁵¹ M. Zielinski,⁵¹ D. Zieminska,³⁷ A. Zieminski,³⁷ V. Zutshi,⁵¹ E. G. Zverev,²² and A. Zylberstein¹²

(D0 Collaboration)

- ¹*Universidad de Buenos Aires, Buenos Aires, Argentina*
²*LAFEX, Centro Brasileiro de Pesquisas Físicas, Rio de Janeiro, Brazil*
³*Universidade do Estado do Rio de Janeiro, Rio de Janeiro, Brazil*
⁴*Institute of High Energy Physics, Beijing, People's Republic of China*
⁵*Universidad de los Andes, Bogotá, Colombia*
⁶*Charles University, Prague, Czech Republic*
⁷*Institute of Physics, Academy of Sciences, Prague, Czech Republic*
⁸*Universidad San Francisco de Quito, Quito, Ecuador*
⁹*Institut des Sciences Nucléaires, IN2P3-CNRS, Université de Grenoble 1, Grenoble, France*
¹⁰*CPPM, IN2P3-CNRS, Université de la Méditerranée, Marseille, France*
¹¹*LPNHE, Universités Paris VI and VII, IN2P3-CNRS, Paris, France*
¹²*DAPNIA/Service de Physique des Particules, CEA, Saclay, France*
¹³*Panjab University, Chandigarh, India*
¹⁴*Delhi University, Delhi, India*
¹⁵*Tata Institute of Fundamental Research, Mumbai, India*
¹⁶*Seoul National University, Seoul, Korea*
¹⁷*CINVESTAV, Mexico City, Mexico*
¹⁸*FOM-Institute NIKHEF and University of Amsterdam/NIKHEF, Amsterdam, The Netherlands*
¹⁹*University of Nijmegen/NIKHEF, Nijmegen, The Netherlands*
²⁰*Institute of Nuclear Physics, Kraków, Poland*
²¹*Institute for Theoretical and Experimental Physics, Moscow, Russia*
²²*Moscow State University, Moscow, Russia*
²³*Institute for High Energy Physics, Protvino, Russia*
²⁴*Lancaster University, Lancaster, United Kingdom*
²⁵*University of Arizona, Tucson, Arizona 85721*
²⁶*Lawrence Berkeley National Laboratory and University of California, Berkeley, California 94720*
²⁷*University of California, Davis, California 95616*
²⁸*California State University, Fresno, California 93740*
²⁹*University of California, Irvine, California 92697*
³⁰*University of California, Riverside, California 92521*
³¹*Florida State University, Tallahassee, Florida 32306*
³²*University of Hawaii, Honolulu, Hawaii 96822*
³³*Fermi National Accelerator Laboratory, Batavia, Illinois 60510*
³⁴*University of Illinois at Chicago, Chicago, Illinois 60607*
³⁵*Northern Illinois University, DeKalb, Illinois 60115*
³⁶*Northwestern University, Evanston, Illinois 60208*
³⁷*Indiana University, Bloomington, Indiana 47405*
³⁸*University of Notre Dame, Notre Dame, Indiana 46556*
³⁹*Iowa State University, Ames, Iowa 50011*
⁴⁰*University of Kansas, Lawrence, Kansas 66045*
⁴¹*Kansas State University, Manhattan, Kansas 66506*
⁴²*Louisiana Tech University, Ruston, Louisiana 71272*
⁴³*University of Maryland, College Park, Maryland 20742*
⁴⁴*Boston University, Boston, Massachusetts 02215*
⁴⁵*Northeastern University, Boston, Massachusetts 02115*
⁴⁶*University of Michigan, Ann Arbor, Michigan 48109*
⁴⁷*Michigan State University, East Lansing, Michigan 48824*
⁴⁸*University of Nebraska, Lincoln, Nebraska 68588*
⁴⁹*Columbia University, New York, New York 10027*
⁵⁰*New York University, New York, New York 10003*
⁵¹*University of Rochester, Rochester, New York 14627*
⁵²*State University of New York, Stony Brook, New York 11794*
⁵³*Brookhaven National Laboratory, Upton, New York 11973*
⁵⁴*Langston University, Langston, Oklahoma 73050*
⁵⁵*University of Oklahoma, Norman, Oklahoma 73019*
⁵⁶*Brown University, Providence, Rhode Island 02912*
⁵⁷*University of Texas, Arlington, Texas 76019*
⁵⁸*Texas A&M University, College Station, Texas 77843*
⁵⁹*Rice University, Houston, Texas 77005*
⁶⁰*University of Washington, Seattle, Washington 98195*

(Received 15 August 2000)

Bottom-quark production in $\bar{p}p$ collisions at $\sqrt{s} = 1.8$ TeV is studied with 5 pb^{-1} of data collected in 1995 by the D0 detector at the Fermilab Tevatron Collider. The differential production cross section for b jets in the central rapidity region ($|y^b| < 1$) as a function of jet transverse energy is extracted from a muon-tagged jet sample. Within experimental and theoretical uncertainties, D0 results are found to be higher than, but compatible with, next-to-leading-order QCD predictions.

PACS numbers: 14.65.Fy, 12.38.Qk, 13.85.Qk

Measurements of the bottom-quark production cross section at $\bar{p}p$ colliders provide an important quantitative test of quantum chromodynamics (QCD). The mass of the b quark is considered large enough ($m_b \gg \Lambda_{\text{QCD}}$) to justify perturbative expansions in the strong coupling constant α_s . Consequently, data on b quark production are expected to be adequately described by calculations at next-to-leading order (NLO) in α_s [1–3].

Past measurements of inclusive b quark production in the central rapidity region, at center-of-mass energies $\sqrt{s} = 0.63$ TeV [4,5] and $\sqrt{s} = 1.8$ TeV [6–9], indicate a general agreement in shape with the calculated transverse momentum (p_T) spectrum, but are systematically higher than the NLO QCD predictions [1–3] by roughly a factor of 2.5. More recently, a measurement using muons at high rapidity [10] ($2.4 < |y^\mu| < 3.2$) to tag b quarks, indicates an even larger excess of observed cross section over theory. The measured differential production cross section for B mesons [11] is similarly higher than the NLO QCD prediction. Calculations of higher order corrections [12,13] have shown that additional enhancements to the cross section beyond NLO are likely. However, the expected enhancements fall short of accounting for the observed discrepancy between theory and data. This long-standing mismatch has motivated continuous theoretical and experimental effort dedicated to reduce uncertainties in general, and to broaden the scope of observable quantities [9,14].

Previous studies of b quark production by the D0 Collaboration have exploited the kinematic relationship between b quarks and daughter (semileptonic decay) muons to extract integrated b quark production rates as a function of p_T^b threshold [7], and have examined azimuthal correlations between the b and \bar{b} in pair production [9].

The present study is a complementary measurement of b production, based primarily on calorimetry, with the main focus being on b jets rather than b quarks. b jets are defined as hadronic jets carrying b flavor. As opposed to quarks, jets are directly observable and therefore reduce model dependence when comparing experimental data with theory. This measurement is in direct correspondence with a NLO QCD calculation [15] that highlights the advantages of considering b jets rather than open b quarks. For instance, large logarithms that appear at all orders in the open quark calculation (due to hard collinear gluons) are avoided when all fragmentation modes are integrated.

The differential production cross section of b jets as a function of the jet transverse energy (E_T) has been measured using data collected during 1995 with the D0 detector

at the Fermilab Tevatron Collider. The data correspond to an integrated luminosity of $(5.2 \pm 0.3) \text{ pb}^{-1}$. The analysis exploits the semileptonic decays of b hadrons which result in a muon associated with a jet. An inclusive sample of muon-tagged jets is selected from a trigger requiring a jet and a muon, and the b jet component of the inclusive sample is extracted, based on the properties expected of the associated muon and jet.

The D0 detector and trigger system are described elsewhere [16]. Jet detection utilizes primarily the uranium-liquid argon calorimeters, which have full coverage for pseudorapidity [17] $|\eta| \leq 4$, and are segmented into towers of $\Delta\eta \times \Delta\phi = 0.1 \times 0.1$, where ϕ is the azimuthal angle. The relative energy resolution for jets is approximately $80\%/\sqrt{E(\text{GeV})}$. The central muon system consists of three layers of proportional drift tubes and a magnetized iron toroid located between the first two layers. The muon detectors provide a measurement of the muon momentum with a resolution parametrized by $\delta(1/p) = \sqrt{[0.18(p-2)/p^2]^2 + (0.003)^2}$, with p in GeV/ c . The total thickness of the calorimeter and toroid in the central region varies from 13 to 15 interaction lengths, which reduces the hadronic punchthrough for the muon system to less than 0.5% of muons from all sources.

Initial event selection used a trigger requiring (i) $E_T > 10$ GeV in at least one calorimeter trigger tile of $\Delta\eta \times \Delta\phi = 0.8 \times 1.6$, (ii) at least one muon candidate with $p_T > 3$ GeV/ c , and (iii) a single $\bar{p}p$ interaction per beam crossing as signaled by the trigger scintillation hodoscopes.

Jet candidates were reconstructed off-line with an iterative fixed-cone algorithm (cone radius of 0.7 in η - ϕ space) and then subjected to quality selection criteria to eliminate background from isolated noisy calorimeter cells and accelerator beam losses which may mimic jets. Accepted jets were required to have $E_T > 25$ GeV, $|\eta| < 0.6$, and an associated muon within the reconstruction cone.

Off-line muon selection required the triggered track to originate from the reconstructed event vertex, with $p_T^\mu > 6$ GeV/ c and $|\eta^\mu| < 0.8$. Muon candidates in the azimuth region $80^\circ < \phi^\mu < 110^\circ$ were excluded due to poor chamber efficiencies near where the main ring beam pipe passes through D0.

Background events from cosmic ray muons were eliminated by requiring a 10 ns wide time coincidence of muon tracks with beam crossings. About 30 000 events were selected, of which less than 0.5% have either a second muon-tagged jet or a double-tagged one. This is in agreement with expectations from muon cuts and acceptance, branching fractions, and flavor content of the sample.

The differential b jet cross section as a function of jet E_T is extracted from the inclusive tagged jet sample as

$$\frac{d\sigma}{dE_T^{b\text{Jet}}} = \frac{U(E_T)F_b(E_T)}{2B\mathcal{L}_{\text{int}}\epsilon^{\mu J}(p_T^\mu, E_T)A(E_T)} \frac{\Delta N^{\mu J}}{\Delta E_T}, \quad (1)$$

where $\Delta N^{\mu J}/\Delta E_T$ represents the inclusive tagged jet counts per transverse energy bin width, $F_b(E_T)$ is the fraction of tagged jets containing muons from b quark decays, $\epsilon^{\mu J}(p_T^\mu, E_T)$ is the event detection efficiency of a $\mu + \text{jet}$ pair, $U(E_T)$ corrects for spectrum smearing from jet energy resolution, $A(E_T)$ corrects for the muon tagging acceptance, \mathcal{L}_{int} is the integrated luminosity of the data sample, and $B = 0.108 \pm 0.005$ is the branching fraction for inclusive decays $b \rightarrow \mu + X$ [18]. Tagging muons of both charges are counted, and the number of events is divided by 2. The cross section is determined for the $(b + \bar{b})/2$ combination. In Eq. (1) and throughout this paper, E_T represents the calorimeter-only component of the jet transverse energy: it excludes the tagging muon and associated neutrino. Once the correction for the lepton energy is included (see below), then $E_T^{b\text{Jet}}$ measures the complete b jet.

The trigger and off-line reconstruction efficiencies were determined from Monte Carlo events, and cross-checked with appropriate control samples of collider data. Monte Carlo events were generated with ISAJET [19], followed by a GEANT [20] simulation of the D0 detector response, trigger simulation, and reconstruction. The overall muon geometric acceptance multiplied by efficiency increases from 35% at $p_T^\mu = 6$ GeV/ c to a plateau of 45% above 10 GeV/ c . The overall jet efficiency increases from 85% at $E_T = 25$ GeV to a plateau of 97% above 45 GeV.

The transverse energy of each jet was corrected for the underlying event, additional interactions, noise from uranium decay, the fraction of particle energy showered outside the jet cone, detector uniformity, and detector hadronic response [21]. The steeply falling E_T spectrum is distorted by jet energy resolution, and was corrected as described in [22].

In addition to b production, muon-tagged jets can also arise from semileptonic decays of c quarks, and in-flight decays of π or K mesons. Muons from Drell-Yan or on-shell W/Z boson production are not expected to have associated jets, and Monte Carlo estimates confirm a negligible contribution. The background from light flavors is suppressed using the transverse momentum of the muon relative to the associated jet axis (p_T^{rel}) as discriminator. The higher mass of the decaying b quark generates a rather different p_T^{rel} distribution than obtained from quark decays of lighter flavor.

Individual p_T^{rel} distributions for muons from b , c (direct), c (sequential from b), and π/K decays were modeled using the ISAJET [19] Monte Carlo, with individual samples of each mode processed through complete detector, trigger, and off-line simulation. Because of the similarity of p_T^{rel} for c and π/K sources, within resolution

these distributions were indistinguishable. The b jet signal was extracted on a statistical basis, through maximum likelihood fits to the observed p_T^{rel} distribution. The normalizations of Monte Carlo templates representing light (c and π/K) and heavy (b) quark decay patterns were floated such as to fit the observed p_T^{rel} spectra in four ranges of transverse energy. The extracted fraction of b jets in each E_T range is shown in Fig. 1. The systematic uncertainties were estimated by varying within errors the input distributions to the maximum likelihood fits.

The parametrization of the overall fraction of b jets in the inclusive sample as a function of jet E_T was obtained from a two-parameter fit ($\chi^2 = 0.96$) to the four bins in E_T , and is shown in Fig. 1, together with the uncertainty band (6% relative uncertainty at 30 GeV, 39% at 100 GeV). The form $(\alpha + \beta/E_T^2)$ was chosen after Monte Carlo fit trials. There are partial bin-to-bin correlations in the uncertainty. The extracted b fraction is the dominant source of uncertainty in the cross section. The upper reach in b jet E_T is limited by the deteriorating discrimination power of p_T^{rel} with increasing E_T .

Corrections for acceptance loss stem from (i) the tagging threshold for muon p_T and range of pseudorapidity, (ii) the muon-jet association (tag) criterion, (iii) the undetected lepton energy of the jet, which is added (statistically) to the hadronic E_T registered in the calorimeter, and (iv) the restricted pseudorapidity range for jets and muons (theory [15] considers b jets with $|\eta| < 1$).

The acceptance correction is extracted using the ISAJET [19] Monte Carlo simulation, and is defined as the ratio of b jets satisfying the analysis conditions to b jets satisfying the cross section definition. The transition from E_T to $E_T^{b\text{Jet}}$ is thus included in the correction. The simulated E_T and η distributions are in agreement with the data. The overall correction increases from 6% at $E_T = 30$ GeV to 10% at 100 GeV. It is independent of assumed event production rates, and is affected primarily by models for fragmentation and decay. Decays are based on the QQ [23] software package from the CLEO experiment. ISAJET uses the Peterson fragmentation model [24], with a parameter

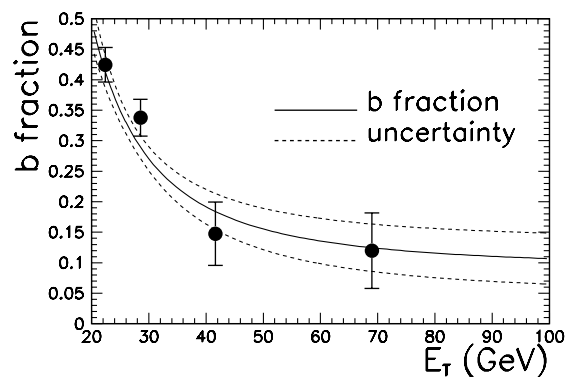
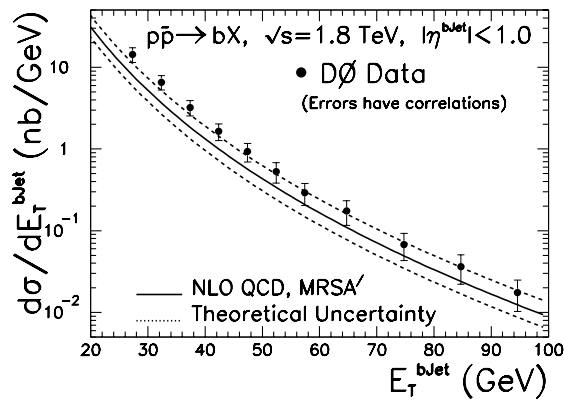


FIG. 1. Fraction of muon-tagged jets which come from b decays. E_T is the calorimeter-only component (see text) of the b jet transverse energy.

FIG. 2. Differential cross section for b jet production.

$\epsilon = 0.006$ that is varied by $\pm 50\%$ to estimate uncertainty. It is observed that the impact of fragmentation on the acceptance is mainly due to the migration of tagging muons across the minimum- p_T boundary. This uncertainty propagates to the cross section as a 9% effect independent of jet E_T .

The resulting b jet cross section for $|\eta| < 1$ is shown in Fig. 2, together with the NLO QCD prediction [15]. Inputs to this calculation are the renormalization scale (chosen equal to the factorization scale), the b quark pole mass ($4.75 \text{ GeV}/c^2$), the parton distribution function (MRSA' [25]), and the parton clustering algorithm. The uncertainty in theory is dominated by the QCD renormalization scale dependence, with the central value in Fig. 2 chosen as $\mu_0 = (E_T^2 + M_b^2)^{1/2}$, and varied between $2\mu_0$ (lower curve) and $\mu_0/2$. The fact that there is such a strong dependence on scale suggests that important higher-order terms in the calculation are still missing.

The overall systematic uncertainty in the cross section has contributions from the integrated luminosity (5%), trigger (3%), and off-line selection (4%) efficiencies, jet E_T scale (15%–8%) and resolution effects (7%–3%), tagging acceptance (9%–12%), and the extracted b fraction of jets (6%–39%). Bin-to-bin errors are fully correlated for all sources of uncertainty, except for partial correlations in the b fraction of jets. Cross section values and overall uncertainties, as plotted in Fig. 2, are listed in Table I.

Figure 2 displays the same general pattern of past b production measurements [4–11], with data lying above the central values of the prediction, but comparatively less so in the present case, where general agreement between measurement and the upper band of the theoretical uncertainty is observed.

To connect the present measurement with previous findings, and in particular the apparent difference in normalization with respect to theory, the present data sample (muon-tagged jets) can be reanalyzed from a different perspective. Instead of focusing on the differential b jets cross section, the same data can be used to reproduce the integrated b quark cross section as a function of minimum p_T^b . Similar measurements are described in Refs. [4–7] and [9]. The kinematic relationship between daughter muons

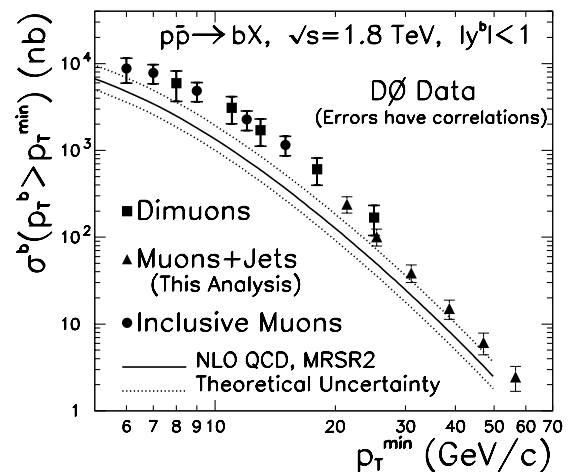
TABLE I. Differential cross section for b jet production.

E_T^{bjet} (GeV)	$d\sigma/dE_T^{bjet}$ (nb/GeV)	Uncertainties (%)	
		Stat.	Syst.
27.3	14.4	1.2	20.6
32.3	6.57	1.6	20.1
37.4	3.22	2.1	21.2
42.4	1.65	2.7	23.2
47.4	0.932	3.4	25.6
52.4	0.530	4.2	28.0
57.4	0.292	5.4	30.2
64.7	0.174	4.6	33.2
74.7	0.0678	6.8	36.6
84.7	0.0364	8.7	39.3
94.6	0.0176	11.7	41.5

(p_T^μ spectrum) and parent b quarks (p_T^b spectrum) is used to extract the b quark production cross section, integrated from p_T^{\min} to infinity, and over the rapidity range $|y^b| < 1$. Here p_T^{\min} is defined as the allowed p_T threshold for a given p_T^μ distribution. Since the b quark signal fraction increases with muon p_T (decreases with jet E_T), b tagging based on p_T^{re1} as a function of p_T^μ is more precise than as a function of jet E_T . The model dependence, introduced in the conversion of the muon p_T spectrum to the integrated b quark spectrum, dominates the uncertainty in this measurement.

The results of this reanalysis are shown in Fig. 3 (triangles) along with the theoretical expectation [1] and the previous D0 [9] results. Consistency among all measurements is evident. The present analysis extends significantly the p_T^b reach of the previous measurements. This is due to the requirement of jets in the trigger and off-line selection, as opposed to requiring just muon triggers. The jet requirement naturally forces the sample into a higher region of p_T^b . Figure 3 shows that the agreement between data and theory improves somewhat at higher p_T^b .

In conclusion, two distinct measurements of b quark production in a previously unexplored region of larger transverse momenta have been presented, and are found to be compatible with the NLO QCD calculation for

FIG. 3. Integrated cross section for b quark production.

heavy-flavor production. Agreement between data and theory, unsatisfactory for previous measurements, is now observed to improve at higher transverse momenta.

We thank the staffs at Fermilab and at collaborating institutions for contributions to this work, and acknowledge support from the Department of Energy and National Science Foundation (U.S.A.), Commissariat à L'Energie Atomique and CNRS/Institut National de Physique Nucléaire et de Physique des Particules (France), Ministry for Science and Technology and Ministry for Atomic Energy (Russia), CAPES and CNPq (Brazil), Departments of Atomic Energy and Science and Education (India), Colciencias (Colombia), CONACyT (Mexico), Ministry of Education and KOSEF (Korea), CONICET and UBACyT (Argentina), A. P. Sloan Foundation, and the A. von Humboldt Foundation.

-
- [1] P. Nason, S. Dawson, and R. K. Ellis, Nucl. Phys. **B327**, 49 (1989); **B335**, 260(E) (1990).
- [2] W. Beenakker *et al.*, Nucl. Phys. **B351**, 507 (1991).
- [3] M. Mangano, P. Nason, and G. Ridolfi, Nucl. Phys. **B373**, 295 (1992).
- [4] UA1 Collaboration, C. Albajar *et al.*, Z. Phys. C **61**, 41 (1994).
- [5] F. Stichelbaut, in *Proceedings of the XXXII Rencontres de Moriond (QCD)*, edited by J. Tran Thanh Van (Editions Frontieres, Gif-sur-Yvette, France, 1997), p. 126.
- [6] CDF Collaboration, F. Abe *et al.*, Phys. Rev. Lett. **71**, 2396 (1993).
- [7] D0 Collaboration, S. Abachi *et al.*, Phys. Rev. Lett. **74**, 3548 (1995).
- [8] D0 Collaboration, S. Abachi *et al.*, Phys. Lett. B **370**, 239 (1996).
- [9] D0 Collaboration, B. Abbott *et al.*, Phys. Lett. B **487**, 264 (2000).
- [10] D0 Collaboration, B. Abbott *et al.*, Phys. Rev. Lett. **84**, 5478 (2000).
- [11] CDF Collaboration, F. Abe *et al.*, Phys. Rev. Lett. **75**, 1451 (1995).
- [12] F. I. Olness, R. J. Scalise, and Wu-Ki Tung, Phys. Rev. D **59**, 14 506 (1999).
- [13] M. Cacciari and M. Greco, Phys. Rev. D **55**, 7134 (1997); Nucl. Phys. **B421**, 530 (1994).
- [14] CDF Collaboration, F. Abe *et al.*, Phys. Rev. D **53**, 1051 (1996); **55**, 2546 (1997); **61**, 32001 (2000).
- [15] S. Frixione and M. Mangano, Nucl. Phys. **B483**, 321 (1997).
- [16] D0 Collaboration, S. Abachi *et al.*, Nucl. Instrum. Methods Phys. Res., Sect. A **338**, 185 (1994).
- [17] The pseudorapidity is defined as $\eta \equiv -\ln(\tan(\theta/2))$, where θ is the polar angle relative to the proton beam.
- [18] Particle Data Group, C. Caso *et al.*, Eur. Phys. J. C **3**, 41 (1998).
- [19] F. Paige and S. Protopopescu, BNL Report No. BNL38034, 1986 (unpublished). Version used is 7.37.
- [20] F. Carminati *et al.*, GEANT Users Guide, v 3.15, CERN Program Library, 1991 (unpublished).
- [21] D0 Collaboration, B. Abbott *et al.*, Nucl. Instrum. Methods Phys. Res., Sect. A **424**, 352 (1999).
- [22] D0 Collaboration, B. Abbott *et al.*, Phys. Rev. Lett. **82**, 2451 (1999).
- [23] <http://www.lns.cornell.edu/public/CLEO/soft/QQ> (unpublished).
- [24] C. Peterson *et al.*, Phys. Rev. D **27**, 105 (1983); J. Chrin, Z. Phys. C **36**, 163 (1987).
- [25] A. D. Martin, R. G. Roberts, and W. J. Stirling, Phys. Lett. B **354**, 155 (1995).